Latcripin-7A, derivative of *Lentinula edodes* C$_{91-3}$, reduces migration and induces apoptosis, autophagy, and cell cycle arrest at G$_1$ phase in breast cancer cells

Syed Riaz Ud Din[1] · Mintao Zhong[1] · Muhammad Azhar Nisar[2] · Muhammad Zubair Saleem[3] · Akbar Hussain[1] · Kavish H. Khinsar[1] · Shahid Alam[4] · Gohar Ayub[5] · Sadia Kanwal[6] · Xingyun Li[1] · Wei Zhang[1] · Xiaoli Wang[1] · Anhong Ning[1] · Jing Cao[1] · Min Huang[1]

Abstract

Due to the high mortality rate and an increase in breast cancer incidence, it has been challenging for researchers to come across an effective chemotherapeutic strategy with minimum side effects. Therefore, the need for the development of effective chemotherapeutic drugs is still on the verge. Consequently, we approached a new mechanism to address this issue. The naturally available peptide named latcripin-7A (LP-7A), extracted from a mushroom called *Lentinula edodes*, provided us promising results in terms of growth arrest, apoptosis, and autophagy in breast cancer cells (MCF-7 and MDA-MB-231). Expressions of protein markers for apoptosis, autophagy, and cell cycle were confirmed via Western blot analysis. Migration and invasion assays were performed to analyze the anti-migratory and anti-invasive properties of LP-7A, while cell cycle analysis was performed via flow cytometry to evaluate its affect over cell growth. Supportive assays were performed like acridine orange, Hoechst 33258 stain, DNA fragmentation, and mitochondrial membrane potential (MMP) to further confirm the anticancer effect of LP-7A on breast cancer cell lines. It is concluded that LP-7A effectively reduces migration and promotes apoptosis as well as autophagy in MCF-7 and MDA-MB-231 breast cancer cell lines by inducing cell growth arrest at G$_0$/G$_1$ phase and decreasing mitochondrial membrane potential without adverse effects on MCF-10A normal breast cells.

Key points

- *In this study, we have investigated the anti-cancer activity of novel latcripin-7A (LP-7A), a protein extracted as a result of de novo characterization of Lentinula edodes C$_{91-3}$.*
- *We conclude in our research work that LP-7A can initiate diverse cell death-related events, i.e., apoptosis and autophagy in both triple-positive and triple-negative breast cancer cell lines by interacting with different nodes of cellular signaling that can further be investigated in vivo to gain a better understanding.*

Syed Riaz Ud Din and Mintao Zhong contributed equally to this work.

✉ Min Huang
  huangminchao@163.com

[1] Department of Microbiology, College of Basic Medical Sciences, Dalian Medical University, Dalian, People's Republic of China

[2] Department of Biochemistry and Molecular Biology, College of Basic Medical Sciences, Dalian Medical University, Dalian, People's Republic of China

[3] Department of Pathology and Pathophysiology, College of Basic Medical Sciences, Dalian Medical University, Dalian, People's Republic of China

[4] Department of Anatomy, Dalian Medical University, Dalian, People's Republic of China

[5] Second Affiliated Hospital of Dalian Medical University, Dalian Medical University, Dalian, People's Republic of China

[6] Department of Biotechnology College of Basic Medical Sciences , Dalian Medical University , Dalian, People's Republic of China

Introduction

In the last decade, we have observed the upscaling in cancer research influenced by several factors. Almost all cancer types got immerse attention in the field of cancer research due to their limitations for diagnosis and treatment. We have seen an intensification in cancer diagnosis over the last few years; however, the rapid increase in the diagnosis of breast cancer got our attention to address this issue effectively. It has been reported that every year positive breast cancer diagnosis contributes to the increase in the number of cases exponentially estimated to cross over a million per year in breast cancer, which is 23% of total cases. Among these, it has been estimated that 18% of the overall cancer cases lead to death (Ballazhi et al. 2017; Porter 2008). The rate of breast cancer is higher in almost every part of the world, including Australia, North America, Asia, and Western Europe (Ferlay et al. 2010). In China, however, this rate of incidence has been increasing since the last few decades from 20 to 30% and counts on rising 3–5% per year, which accounts for a global increase in 1.5% annually (Anderson et al. 2008; Li et al. 2016)

Naturally extracted products are always suggested to be the best choice of treatment with a focus on minimum side effects and higher efficiency (Joseph et al. 2018). Mushrooms have a long history of serving as one of the best candidates to be used as medicine and food sources providing high nutritional values (Jong and Birmingham 1993). One of the well-studied mushrooms is *Lentinula edodes* for its medicinal characteristics such as antimicrobial efficiency, immune stimulator, and anti-cancer activity (Bisen et al. 2010; Jong and Birmingham 1993; Rincao et al. 2012). Clinical trials on *Lentinula edodes'* secondary metabolites as an anti-cancer therapeutic agent have proven to possess the properties to minimize the side effects when combined with traditional chemotherapeutic agents (Jong and Birmingham 1993). Due to such properties, our research team has expressed and isolated several secondary metabolites, including peptides of *Lentinula edodes*, and investigated on several cancer cell lines for their anti-cancer therapeutic efficacy. We have accomplished successful results on growth inhibition of lung cancer cells and gastric cancer cells at G1 phase cell cycle arrest via the treatment of extracted peptides such as latcripin-3 (LP-3) and latcripin-1 (LP-1), respectively, which involved targeting NF-κB signaling for the growth inhibition (Ann et al. 2014; Batool et al. 2018; Liu et al. 2012).

Latcripin-7A (LP-7A), on the other hand, has not been evaluated for its anti-cancer efficacy. Occurrence and abundance of breast cancer over the past decade widely increased the focus of our study on finding the efficiency of LP-7A on

breast cancer cell lines. Therefore, we have simultaneously analyzed breast cancer cells (MCF-7 and MDA-MB-231) and breast normal cells (MCF-10A) to study comparatively the adverse effect of LP-7A in these cells. We have sustained breast cancer cells to further evaluate the mechanistic study for efficacy of LP-7A in detail to establish a baseline for our conclusion.

Materials and methods

Cell culture and reagents

MCF-10A, along with MCF-7 and MDA-MB-231 breast cancer cell lines, were acquired from Shanghai Cell Bank, Chinese Academy of Sciences (Shanghai, China). These cells were maintained and cultured in Dulbecco's Modified Eagle's medium (DMEM) (Cyclone; GE Healthcare Life Sciences, Logan, UT, USA) with 10% fetal bovine serum (FBS), obtained from Tianjin Haoyang Biological Products Technology Co., Ltd., (Tianjin, China), along with penicillin (100 units/mL) and streptomycin (100 μg/mL) at 37 °C, in a humidified atmosphere with 5% CO_2.

MMP-2 (polyclonal, 10373-2-Ap), MMP-9 (polyclonal, 10375-2-Ap), IKB (polyclonal, 10268-1-AP), NF-κB (polyclonal, 14220-1-AP), p21 (polyclonal, 10355-1-Ap), Cdk6 (polyclonal, 14052-1-Ap), cyclin E1 (polyclonal, 11554-1-Ap), cytochrome C (polyclonal, 10993- 1-Ap), Bax (polyclonal, 23931-1-Ap), Bcl-2 (polyclonal, 12789-1-Ap), cleaved caspase-9 (polyclonal, 10380-1-AP), cleaved caspase-1 (polyclonal, 22915-1-AP), caspase-3 (polyclonal, 19677-1-Ap), Atg7 (Monoclonal, 67341-1-Ig), Atg12 (polyclonal, 11122-1-Ap), Atg5 (polyclonal, 10181-2-Ap), LC3 I/II (polyclonal, 12135-1-AP), p62 (polyclonal, 18420-1-AP), and GAPDH along with secondary anti-rabbit antibody were purchased from Proteintech (Wuhan, China). Beclin-1 (monoclonal, ab207612) was purchased from Abcam, while p-IKB (monoclonal, #2859) and caspase-6 (polyclonal, 9762) were obtained from Cell Signaling Technology (USA). Cleaved PARP (monoclonal, k-200,027 M) was purchased from Solarbio Life Sciences. Cyclin D1 (polyclonal, 60186-1-ig) and caspase-8 (monoclonal, 66093-1-ig) were procured from Thermo Fisher Scientific, Waltham, MA, USA). Annexin V-FITC/PI kit and Hoechst 33258 assay kit were obtained from keyGEN BioTECH (Shanghai, China). Matrigel matrix was acquired from Corning Inc. (USA), and acridine orange was obtained from Solar-bio Science & Technology (China).
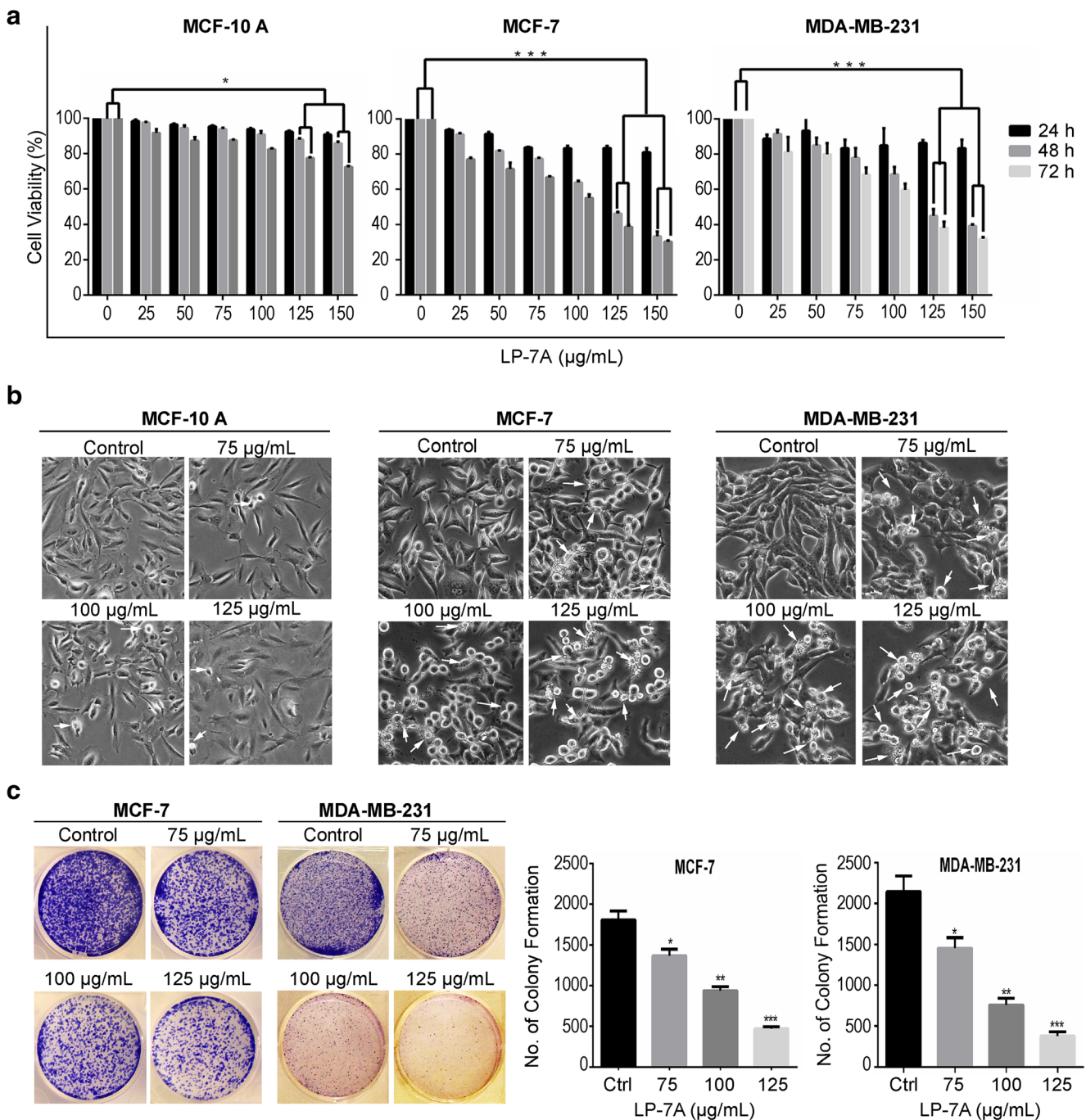
Fig. 1 Breast cancer cell growth inhibition by LP-7A. A Effect of LP-7A, across various concentrations (0-150 μg/mL), on viability, and proliferation of MCF-10A, MCF-7, and MDA-MB-231 was performed via CCK-8. B Morphological changes were observed in MCF-7, MDA-MB-231, and MCF-10A by treating with 75 μg/mL, 100 μg/mL, and 125 μg/mL concentration of LP-7A for 48 h along with a control group, and phase-contrast images were taken at 40X magnification. C Colony morphology was also performed in MCF-7 and MDA-MB-231 with the same concentrations of LP-7A. Statistical analysis via multiple t test was performed using GraphPad Prism 6.0 (* $p < 0.05$, ** $p < 0.01$, *** $p < 0.001$)

Purification and expression of recombinant protein LP-7A

Latcripin-7A (LP-7A) is a registered recombinant protein from *Lentinula edodes* C_{91-3} (China General Microbiological Culture Collection Center; CGMCC no: 7354) with accession number #MT334074. The expression of the active form of LP-7A (39 kDa) was performed following a previously described protocol (Padhiar et al. 2018). Briefly, the LP-7A gene was expressed in *Rosetta gami*

(DE3) using the Pet32a (+) expression vector. The induction of LP-7A was amplified with (isopropyl-β-D-thiogalactopyranoside) IPTG (0.5 mM). Lysis buffer solubilization was performed under various conditions through the freeze-thaw method by using solubilization buffer (50 mM Tris-HCl, 3 M urea pH 7.5. 100 mM NaCl). Further purification was done with anti-His magnetic beads (Bio tool/US) following the manufacturer's protocol. His-tag beads were incubated in binding buffer (20 mM NaH_2PO_4, 500 mM NaCl, 30 mM imidazole, 3 M urea pH 7.5) at 4 °C to activate the beads. Solubilized protein was added, and inclusion bodies (IBs) washing buffer (50 mM Tris-HCl, 100 mM NaCl, 01 mM EDTA, 1% Triton X-100, 3 M urea pH 7.5) was used for washing the His-tag column to remove impurities. Elution of bounded His-tag proteins was eluted by adding elution buffer (20 mM NaH_2PO_4, 500 mM NaCl, 500 mM imidazole, 3 M urea pH 7.5). Refolding was optimized via refolding buffers with pH ranging from 6.0 to 9.0 (Supplementary Table S1), and final purification and concentration were done by dialysis using dialysis buffer (0.238 mM NaHCO3 and 0.38 1 mM EDTA Na2). SDS gel electrophoresis and BCA (bicinchoninic acid) assay were performed in each step for qualitative and quantitative analysis of LP-7A.

Cytotoxicity and cell viability

MCF-10A (4×10^3), MCF-7, and MDA-MB-231 (3×10^3) were cultured in 96-well plate containing 200 μl DMEM. Cells were grown at 37 °C with 5% atmospheric CO_2. Upon 70% confluency, cells were washed gently with PBS and various concentrations of LP-7A (0 μg/mL to 150 μg/mL) were applied as treatment and supplemented with fresh 10% FBS containing DMEM. After 48h treatment, CCK-8 solution (10 μl/well) was supplemented, followed by an incubation period of 3 to 5 h. Upon the change in color, optical density (OD) at 450 nm was analyzed. The growth curve was formulated and inhibitory concentration (IC_{50}) was calculated using GraphPad Prism 6.0.

Phase contrast microscopy and colony formation assay

MCF-7 and MDA-MB-231 breast cancer cells, along with MCF-10A normal breast cells, were treated with indicated concentrations of LP-7A for 48 h. After washing, the cells were re-submerged in DMEM, and phase-contrast images were taken at 40X magnification by using a phase-contrast microscope (Olympus IX53). For colony assay, breast cancer cell lines were treated in the same manner for 48 h. After washing with PBS, cells were trypsinized and transferred into 6-well plates (500 cells per well) along with fresh 2 mL DMEM medium. These 6-well plates were incubated at 37 °C and the growth medium was replaced after every

Fig. 2 LP-7A inhibits migration and invasion in breast cancer cells. **A** Wound healing assay was performed for the migration capability of MCF-7 and MDA-MB-231 under various concentrations of LP-7A (75 μg/mL, 100 μg/mL, 125 μg/mL, and a control group) at a time interval of 0 h, 24 h, and 48 h. **B and C** Furthermore, under the same concentration of LP-7A, both of the breast cancer cell lines, i.e., MCF-7 and MDA-MB-231, were cultured in a trans-well chamber, with Matrigel (Invasion) and without Matrigel (Migration), for the study of migration and invasion. **D** Additionally, migration-related proteins MMP-2 and MMP-9 expressions were evaluated by Western blot under the different doses of LP-7A in MCF-7 and MDA-MB-231 cells. **E** Additionally, proliferation markers IKB, p-IKB, and NF-κB were also evaluated in both of these cell lines via Western blot by treating cells with LP-7A (75 μg/mL, 100 μg/mL, 125 μg/mL and a control (0 μg/mL) indicated as C. Statistical analysis was performed using multiple t test via GraphPad Prism 6.0 (* $p < 0.05$, ** $p < 0.01$)

48 h. Colonies were observed under a period of 10 days. 4% paraformaldehyde (PFA) was used for 15 min to fix the cells and stained with crystal violet dye for 10 to 20 min. These colonies of breast cancer cells, treated with LP-7A, were then washed with PBS. Images were taken by a Sony IMAX Sensor camera.

Wound healing assay

6-well plates were used for the culture of breast cancer cells, and after reaching to desire confluency, a scratch was made in each plate by using a sterilized 10μl pipette tip. After the scratch, cells were washed with PBS three times gently. The indicated concentration of LP-7A was used as a treatment for these breast cancer cells. Cells were incubated at 37 °C and images were taken after the stated time period.

Migration and invasion assay

Cell migration and invasion assay was performed in an 8μm pore-sized transwell chamber (Corning Inc.). Manufacturer instructions were followed for Matrigel dilution and concentration used for invasion. Briefly, after diluting Matrigel, the matrix was allowed to coagulate for 12 h (37 °C) in the transwell chamber plates. LP-7A-treated and LP-7A-untreated cells were then trypsinized and seeded (3×10^3) in a transwell chamber with and without Matrigel for concerned assay. DMEM with 2% FBS was added to the upper chamber, while the lower chamber contained DMEM with 10% FBS. The transwell chamber plate was then incubated at 37 °C for 48 h to initiate the process of migration and invasion from the upper to lower chamber. Cells attached to the inner side of the upper chamber were removed via a soft cotton swab, while the outer lower side of the upper chamber was allowed to fix using 4% PFA for 15 min. Later on, these fixed cells were stained with crystal violet dye. Cells were subjected to a light microscope for imaging at 20X magnification.
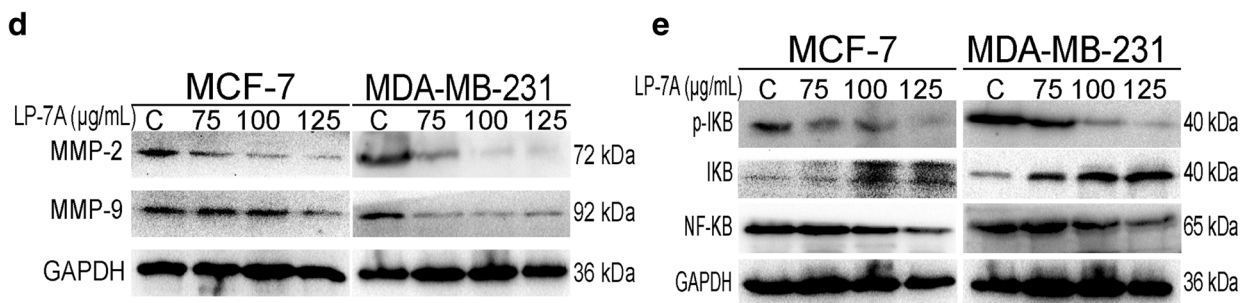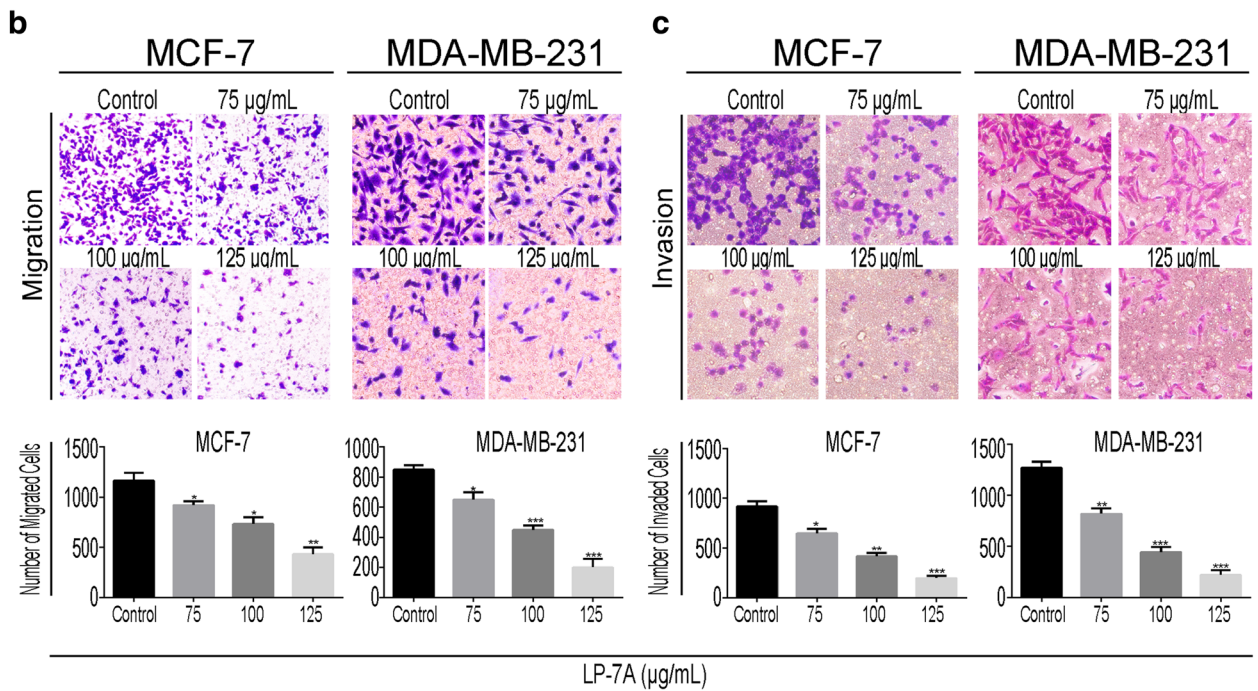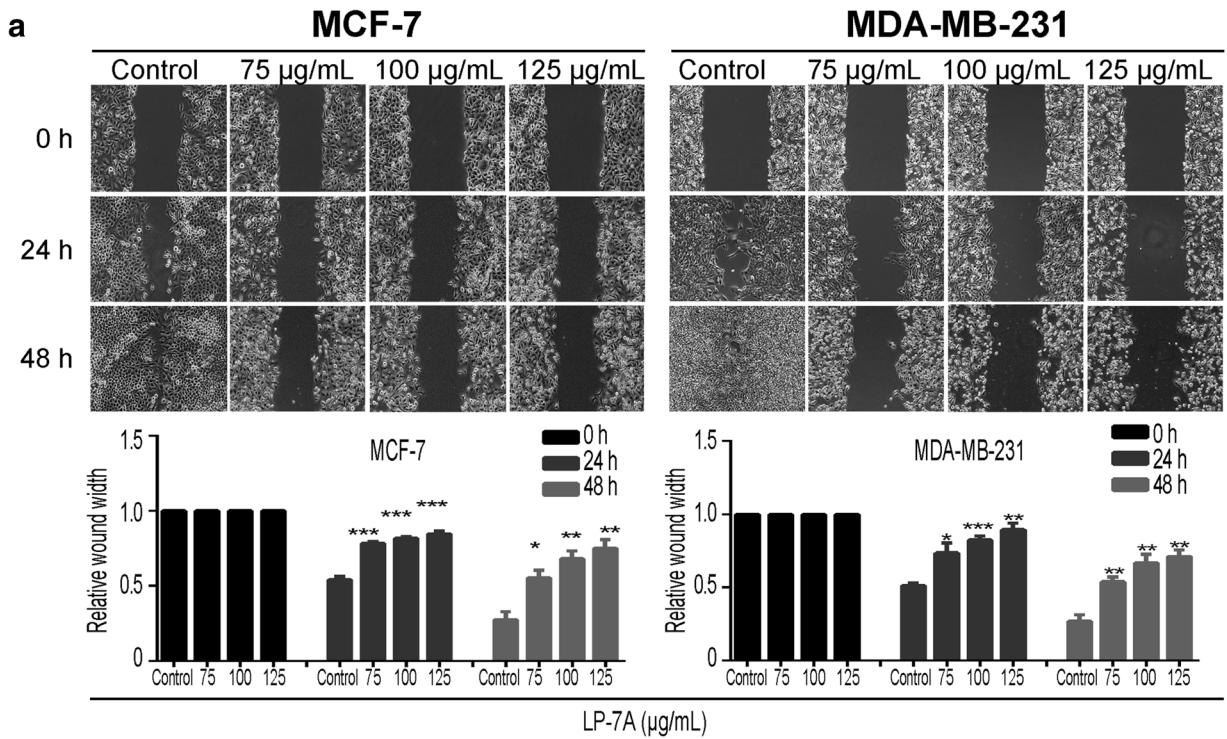
Hoechst 33258 staining

For Hoechst 33258 staining, 12-well plates were used to culture breast cancer cells. Indicated concentrations as treatment of LP-7A were given, as mentioned before, for 48 h. Breast cancer cells were washed with PBS and fixed with 4% PFA. The cells were washed, and 100 µl of Hoechst 33258 stain was applied following the manufacturer's protocol. The washing was repeated to remove the extra stain and cells were exposed to a fluorescent microscope for imaging.

DNA fragmentation assay

LP-7A-treated cells (MCF-7 and MDA-MB-231) were collected after 48 h and washed with PBS. Cell lysis was performed with the lysis buffer provided by the KeyGen DNA fragmentation kit and enzyme treatment was followed. DNA was precipitated by using 70% ethanol, and the DNA was mixed with an equal amount of agarose gel loading buffer to carry out the electrophoresis on 15% agarose gel. Later on, images were taken by the ChemiDoc XRS and Bio-Rad Imaging tool.

Cell cycle analysis

LP-7A-treated breast cancer cells were collected and washed after 48 h with PBS. The cells were subjected to 70% ethanol overnight at 4 °C for fixation. The cells were then collected and centrifuged. Approximately 1×10^6 cells/mL were resuspended in 50 µg/mL propidium iodide (PI) along with 05 µg/mL RNase and then analyzed by FACS-Calibur Cytometer (BD Accuri C^6 Biosciences, Heidelberg, Germany) after incubation for 30 min at 37 °C.

Measurement of mitochondrial membrane potential

Mitochondrial membrane potential (MMP) was analyzed and evaluated using the JC-1 kit (kGA 601) in LP-7A-treated breast cancer cell lines after 48 h of treatment. The manufacturer's protocol was followed. Briefly, cells were washed with PBS, treated with JC-1 solution for 10 min in the dark, and then washed with dilution buffer. The OD at 535 nm was measured using a microplate reader.

Apoptosis by flow cytometry using Annexin-V-FITC/PI staining

LP-7A-treated cells were collected after 48 h and washed with PBS. Cells were collected again and stained with PI and Annexin V-FITC following manufacturer's protocol. The rate of apoptosis was then measured by using FACS-Calibur Cytometer.

Fig. 3 Induction of DNA fragmentation by LP-7A in breast cancer cells. ▶ A Hoechst 33258-stained fluorescent images for the analysis of nuclear morphological changes after 48 h of LP-7A (75 µg/mL, 100 µg/mL, 125 µg/mL compared with control group) treatment at 40X magnification in MCF-7 and MDA-MB-231 cells. B Analysis of DNA fragmentation in MCF-7 and MDA-MB-231 breast cancer cells treated with various concentrations of LP-7A after 48 h. The arrangement of lanes is as follows: lane 1, DNA marker DL10,000; lane 2, 0 µg/mL; lane 3, 75 µg/mL; lane 4, 100 µg/mL; and lane 5, 125 µg/mL of LP-7A. Statistical analysis was perform using multiple t test via GraphPad Prism 6 (* $p < 0.05$, ** $p < 0.01$)

Acridine orange staining

Breast cancer cells treated with LP-7A were washed with PBS three times and collected after 48 h. Cells were then stained with acridine orange as following manufacturer's instructions and kept in the dark for 15 min at 37 °C. Cells were washed with PBS and transferred to glass slides for imaging under a fluorescent microscope (Olympus IX53).

Western blot

LP-7A-treated cells were collected and washed with ice-chilled PBS. Cell lysis was performed by using RIPA (radioimmunoprecipitation assay) reagent supplemented with protease and phosphatase inhibitor (Transgen Biotech, Beijing, China). The lysate was collected and centrifuged for 20 min at a cold temperature. The concentration of protein was determined by using a BCA kit, and 20 to 40 µg/mL of protein per well was loaded on sodium dodecyl sulfate-polyacrylamide gel. Proteins were resolved and separated via sodium dodecyl sulfate-polyacrylamide gel electrophoresis (SDS-PAGE). These were then transferred on a PVDF (polyvinylidene fluoride) membranes (Millipore, Billerica, MA, USA) and blocked for 1 h at room temperature by using a blocking buffer, i.e., 5% skimmed milk in TBST (20 mM Tris-HCl (pH 7.5), 150 mM NaCl, 0.1% Tween 20). Blotted membranes were then incubated with represented antibodies overnight at a dilution followed by the manufacturer's instruction. The next day, membranes were re-incubated with secondary HRP conjugated antibodies for at least 1 h after three times repeated washing with TBST for 15 min at room temperature. Blots were developed using a chemiluminescence detection kit. The membranes were subjected to imaging for analysis, and the ChemiDcoTM XRS + Imager-Bio-Rad imaging tool was used for this purpose.

Statistical analysis

Data analysis was performed by using one-way analysis of variance (ANOVA), and multiple comparison t test was applied by using GraphPad Prism 6.0. All experiments were performed in triplicate unless mentioned otherwise.

a

b
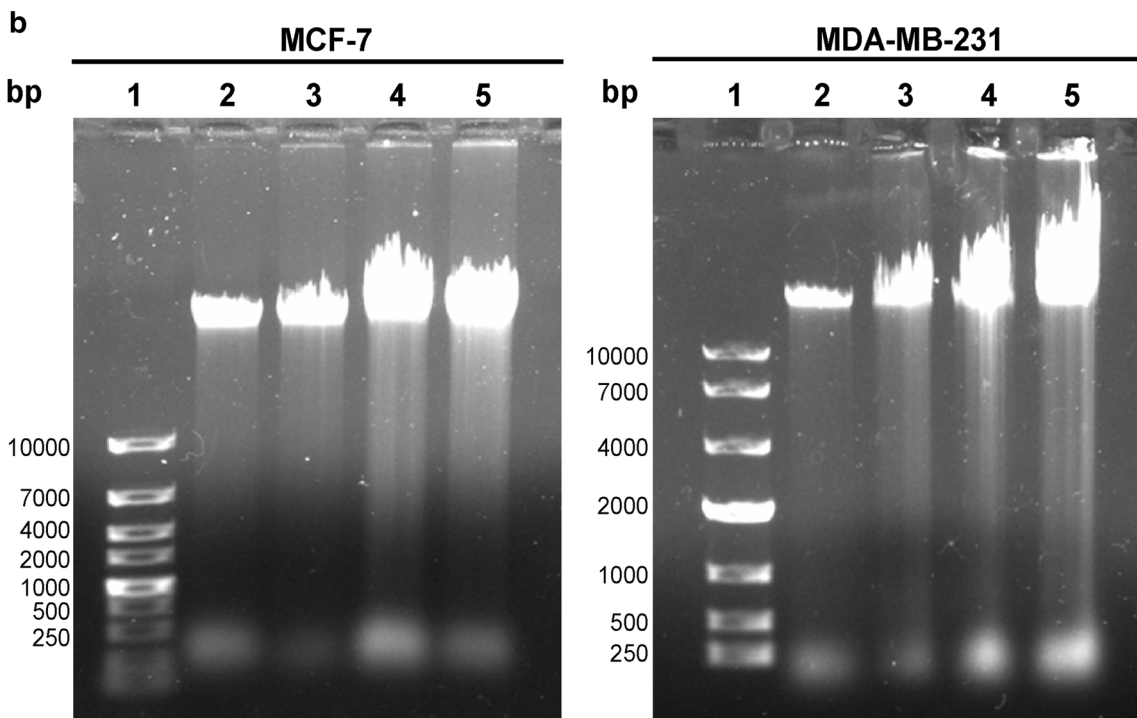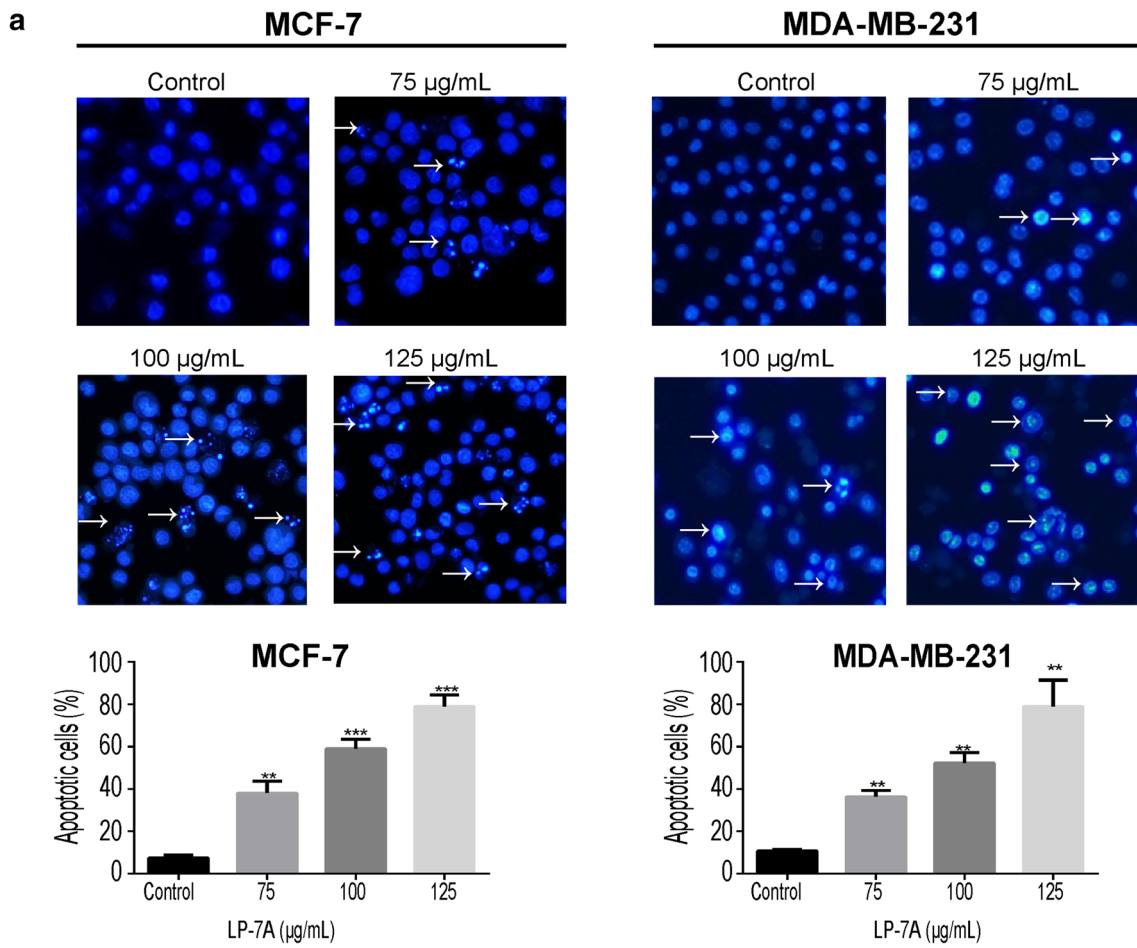
Results

Optimization of expression and purification of LP-7A

LP-7A expression has been carried out in *Rosetta gami* (DE3) using the Pet32a (+) expression vector. It has been found that 6 mM of IPTG provides maximum induction, up to 1.4fold more than the control group, of the expression of Pet32a. The peak induction has been recorded at the 4th h on the time scale (Fig. S1A). The purification has been further improved using a refolding buffer providing maximum solubility at pH 7.5 with − 80 °C temperature (Fig. S1B). These conditions have been utilized before the further purification of LP-7A through His-tag beads to provide maximum productivity of LP-7A (Fig. S1C).

LP-7A inhibits proliferation in breast cancer cells

Cell viability assessment was performed by cytotoxicity assay via CCK-8 kit in two breast cancer cell lines, i.e., MCF-7 and MDA-MB-231, and a breast normal cell line (MCF-10A) with various concentrations ranging from 0 to 150 μg/mL for 48 h. IC_{50} was calculated for all of these cell lines, which was 91 μg/mL for MCF-7 and 122 μg/mL for MDA-MB-231 cell line, while the cytotoxic effect of LP-7A was lower on normal cell line (MCF-10A) with a significantly higher IC_{50} value, i.e., 1.8 mg/mL (Fig. 1A). Due to the high significance of LP-7A in terms of growth arrest in breast cancer cells, we also analyzed morphological changes under phase contrast microscope with three variable doses of LP-7A (75 μg/mL, 100 μg/mL, 125 μg/mL) and a control group without treatment. MCF-7 and MDA-MB-231 breast cancer cells were observed to undergo aggressive deformation after 48 h with the increasing dose of LP-7A treatment, while no significant change in the shape of MCF-10A was observed (Fig. 1B). Since the effect of LP-7A was significantly higher in breast cancer cells, we further evaluated the proliferation of MCF-7 and MDA-MB-231 via colony assay, which showed consistency with our previous CCK-8 results. The number of colonies with the increasing concentrations of LP-7A (75 μg/mL, 100 μg/mL, 125 μg/mL) in MDA-MB-231 and MCF-7 was reduced significantly as compared with the control group (Fig. 1C). These results suggested that LP-7A has a remarkable inhibitory effect on breast cancer cells (MCF-7 and MDA-MB-231), while in breast normal cell (MCF-10A), a lower or negligible impact on growth and proliferation was observed.

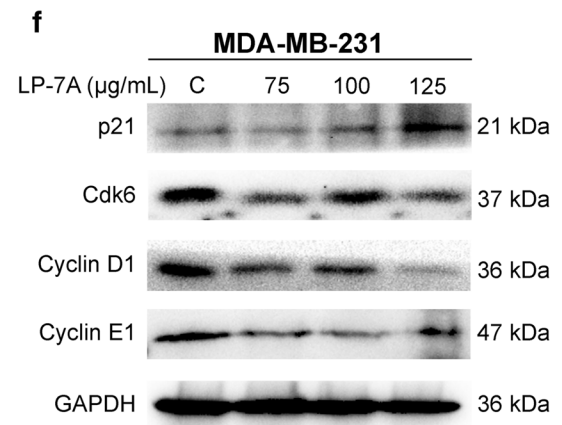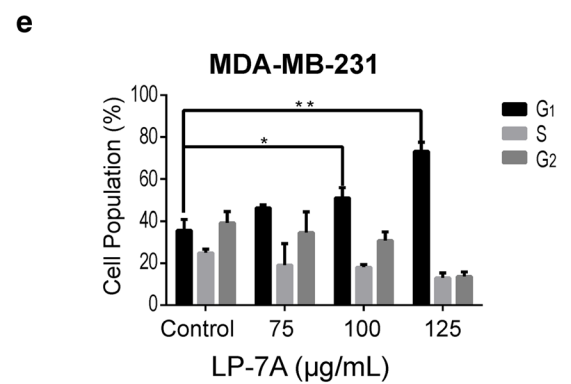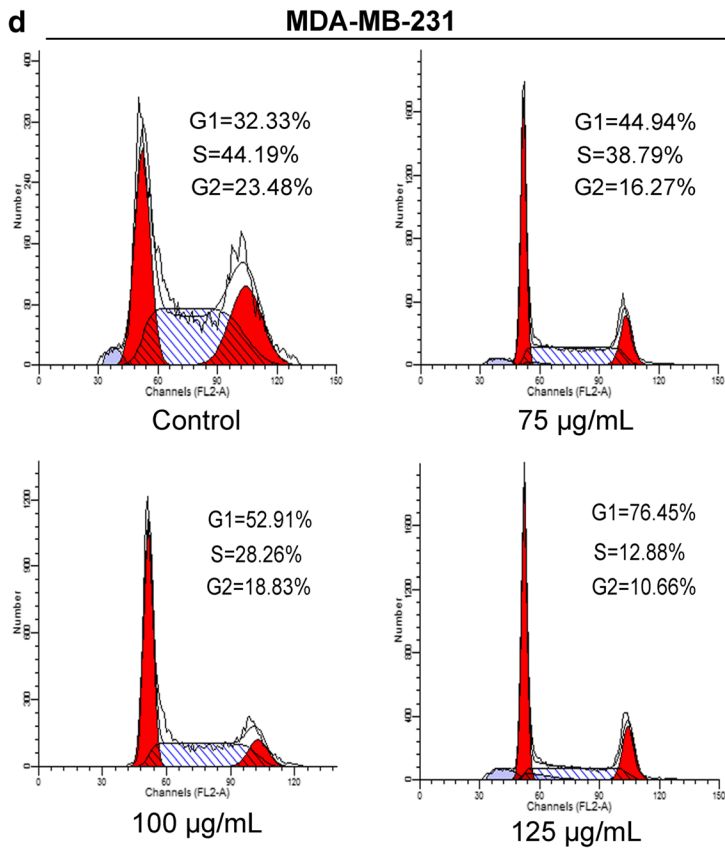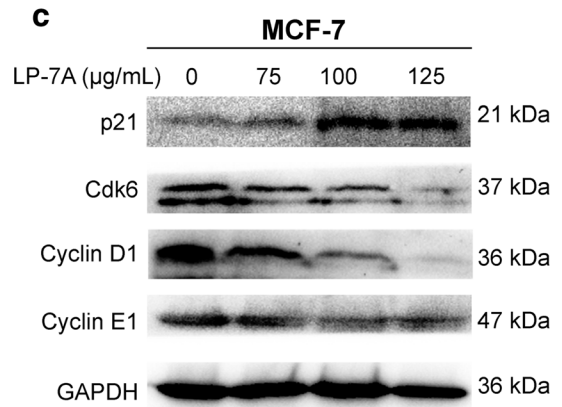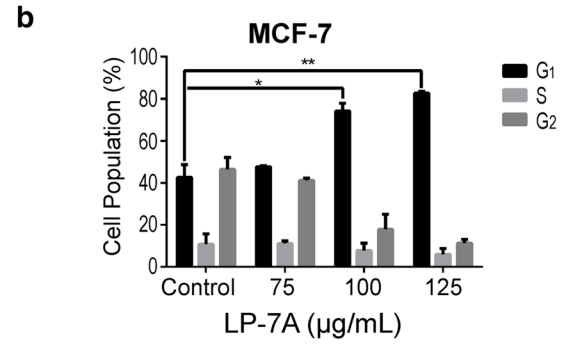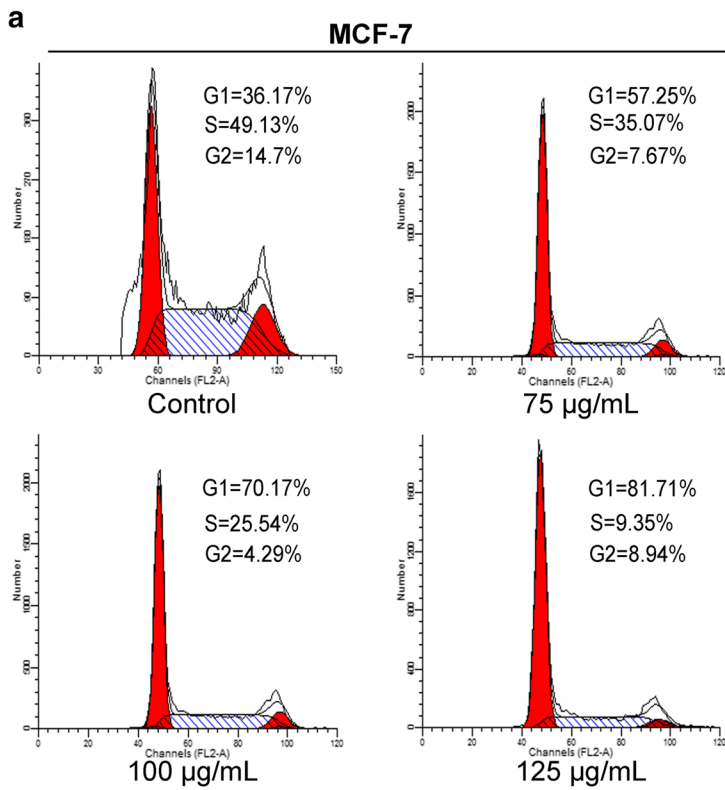## LP-7A inhibits migration and invasion of MCF-7 and MDA-MB-231 cancer cells

Due to the higher growth inhibitory effect of LP-7A in MCF-7 and MDA-MB-231, we evaluated these two cancer cell lines for their migration and invasion capability under LP-7A

Fig. 4 LP-7A induces p21-mediated cell cycle arrest at G_0/G_1 phase. LP-▶ 7A (control, 75 μg/mL, 100 μg/mL, 125 μg/mL)-treated breast cancer cell lines were analyzed for DNA content measurement using a flow cytometer after 48 h. Images are represented in terms of percent distribution of cells into G_0/G_1, S, and G_2 phase in MCF cells (**A and B**) and MDA-MB-231 cells (**D and E**). Additionally, p21, cdk6, cyclin E1, and cyclin D1 expressions were evaluated via Western blot across similar concentrations of LP-7A (control (0 μg/mL) indicated as C, 75 μg/mL, 100 μg/mL, 125 μg/mL) in MCF-7 (**C**) and MDA-MB-231 (**F**). Statistical analysis was performed using multiple *t* test via GraphPad Prism 6 (* $p < 0.05$, ** $p < 0.01$)

treatment. By performing wound healing assay, we observed that MCF-7 and MDA-MB-231 showed a significant decrease in filling the scratched gap between cells under pre-selected doses of LP-7A as indicated before under different time periods, i.e., 0 h, 24 h, and 48 h (Fig. 2A). A similar effect was also observed while performing trans-well chamber assay for migration (without Matrigel layer) and invasion (with Matrigel layer). Cells were treated with the same concentration of LP-7A and allowed to culture on trans-well having an FBS gradient (10% FBS in the lower chamber and 2% in the upper chamber) for 48 h. Both cell lines (MCF-7 and MDA-MB-231) showed a significant decrease in migration (Fig. 2B) and invasion (Fig. 2C) across the trans-well membrane with higher LP-7A treatments. We further confirmed these effects by evaluating the expression of markers such as metalloproteinase-2 (MMP-2) and metalloproteinase-9 (MMP-9) via Western blotting. MMP-2 and MMP-9 were observed to be significantly decreased in MCF-7 and MDA-MB-231 with increasing concentrations of LP-7A (75 μg/mL, 100 μg/mL, 125 μg/mL) as compared with the control group (Fig. 2D). Furthermore, we also analyzed the downstreaming proteins, i.e., p-IKB, IKB, and NF-κB, that can also affect the proliferation, migration, and invasion. The expression of IKB was increased, but the activation of IKB into phosphorylated form was decreased significantly with increasing LP-7A concentration. The expression of NF-κB was also reduced in MCF-7 and MDA-MB-231 cells, with indicated LP-7A treatment (Fig. 2E). These results suggest that the downregulation of MMP-2, MMP-9, and NF-κB along with lower IKB activation (p-IKB) resulted in a decrease in proliferation rate at a cellular level in response to LP-7A.

LP-7A induces DNA fragmentation and nuclear morphological changes in breast cancer cells

Previous reports suggest that apoptotic cells have unique characteristics of nuclear morphology, such as genomic or chromatin condensation, nuclear DNA cleavages, or nuclear membrane rupture (Balasubramanian et al. 2007; Wyllie 1980; Wyllie et al. 1980). To study the role of LP-7A in the nuclear morphological changes and DNA fragmentation, we

a   MCF-7

G1=36.17%
S=49.13%
G2=14.7%

Control

G1=57.25%
S=35.07%
G2=7.67%

75 μg/mL

G1=70.17%
S=25.54%
G2=4.29%

100 μg/mL

G1=81.71%
S=9.35%
G2=8.94%

125 μg/mL

b   MCF-7

c   MCF-7

LP-7A (μg/mL)   0   75   100   125

p21   21 kDa
Cdk6   37 kDa
Cyclin D1   36 kDa
Cyclin E1   47 kDa
GAPDH   36 kDa

d   MDA-MB-231

G1=32.33%
S=44.19%
G2=23.48%

Control

G1=44.94%
S=38.79%
G2=16.27%

75 μg/mL

G1=52.91%
S=28.26%
G2=18.83%

100 μg/mL

G1=76.45%
S=12.88%
G2=10.66%

125 μg/mL

e   MDA-MB-231

f   MDA-MB-231

LP-7A (μg/mL)   C   75   100   125

p21   21 kDa
Cdk6   37 kDa
Cyclin D1   36 kDa
Cyclin E1   47 kDa
GAPDH   36 kDa

performed Hoechst 33258 staining and DNA gel electrophoresis assay, respectively. Nuclear morphological change has been observed in the treated cells of MCF-7 and MDA-MB-231 by staining the nucleus by using Hoechst 33258 stain (Fig. 3A). Furthermore, the extracted DNA of LP-7A-treated cells were also analyzed via electrophoresis on agarose-based gel along with an untreated control group resulting in higher fragmentation with the increasing dose of LP-7A (Fig. 3B). These results suggested the potential role of LP-7A in growth inhibition of breast cancer cells via DNA fragmentation is an intermediate path towards the cell death.

LP-7A induces G_0/G_1 phase cell cycle arrest mediated by p21 in breast cancer cells

Cell cycle analysis of dose-dependent LP-7A-treated breast cancer cell lines showed that a significant number of cells were arrested in G_0/G_1 phase compared with the control group. The trend of increase in the G_1 phase in MCF-7 was 57%, 70%, and 81% at the concentration of 75 μg/mL, 100 μg/mL, and 125 μg/mL, respectively, in comparison with the control group, which was 36%. Moreover, reduction in S phase was also observed i.e., 49%, 35%, 25%, and 9% at the concentration of 0 μg/mL, 75 μg/mL, 100 μg/mL, and 125 μg/mL, respectively (Fig. 4A and B). A similar trend was also found in MDA-MB-231, which showed increase in G_0/G_1 phase (32%, 45%, 53%, and 76%) while decrease in S phase (44%, 39%, 28%, and 13%) across the concentrations of 0 μg/mL, 75 μg/mL, 100 μg/mL, and 125 μg/mL, respectively (Fig. 4D & E). Furthermore, we also confirmed our results by analyzing the expression of cell cycle-related markers through Western blot. It was observed that the inhibitor of cyclin-Cdk complex, i.e., p21, showed higher expression along with a decrease in the expression of Cdk6, cyclin D1, and cyclin E1 in MCF-7 (Fig. 4C) and MDA-MB-231 (Fig. 4F), confirming the inhibition of cell growth with increasing concentration of LP-7A treatment. These results showed that with the treatment of LP-7A, the cancer cell growth inhibition is arrested at G_0/G_1 phase in which the activation of p21 plays an important role.

LP-7A induces mitochondrial -mediated late apoptosis in breast cancer cells

Annexin V-FITC and PI stain, which is commonly used for monitoring the externalization of phosphatidylserine on the cellular membrane as a result of apoptosis, was performed via flow cytometry in LP-7A treated breast cancer cell lines. We found a significant increase in late-stage apoptosis in LP-7A-treated cells as compared with the control group in both breast cancer cells. Treated MCF-7 and MDA-MB-231 also indicated the increase in the induction of necrosis as compared with their control groups (Fig. 5A). Furthermore, higher significant

Fig. 5 Induction of apoptosis by LP-7A in breast cancer cell lines. **A** Flow cytometry was performed for the study of induction of apoptosis by LP-7A-treated MCF-7 and MDA-MB-231 cells with various concentrations (75 μg/mL, 100 μg/mL, 125 μg/mL, and keeping 0 μg/mL as a control group). These treated cells were stained with annexinV-FITC/PI. Quadrant numbers are represented as annexin V+/PI−, (lower right), and annexin V−/PI (lower left) showing early apoptotic and viable cells, respectively, while annexin V+/PI+ (upper right) indicates late apoptosis. **B** Furthermore, expression of apoptotic markers such as Bax/Bcl-2, cytochrome c, and caspases such as cleaved caspase-8, cleaved caspase-9, cleaved caspase-6, and cleaved caspase-1 along with cleaved PARP was evaluated via Western blot in LP-7A (control (0 μg/mL) indicated as C, 75 μg/mL, 100 μg/mL, 125 μg/mL)-treated MCF-7 and MDA-MB-231 cells. **C** Mitochondrial membrane potential (MMP) was analyzed by JC-1 kit in LP-7A (0 μg/mL, 75 μg/mL, 100 μg/mL, 125 μg/mL)-treated breast cancer cell lines. Statistical analysis was performed using multiple t test via GraphPad Prism 6.0 (* $p < 0.05$, ** $p < 0.01$)

upregulation was also observed in mitochondrial-mediated apoptotic marker proteins such as Bax, as well as in cytochrome C, caspase-9, caspase-8, caspase-6, and caspase-1, along with cleaved PARP expression, with increasing dose of LP-7A treatment. In contrast, the expression of Bcl-2 was decreased as compared with the control group (Fig. 5B). These results suggested that intrinsic apoptotic pathways are triggered to initiate apoptosis of breast cancer cells, which was further evaluated by measuring the significant decrease in mitochondrial membrane potential in LP-7A-treated cells (Fig. 5C).
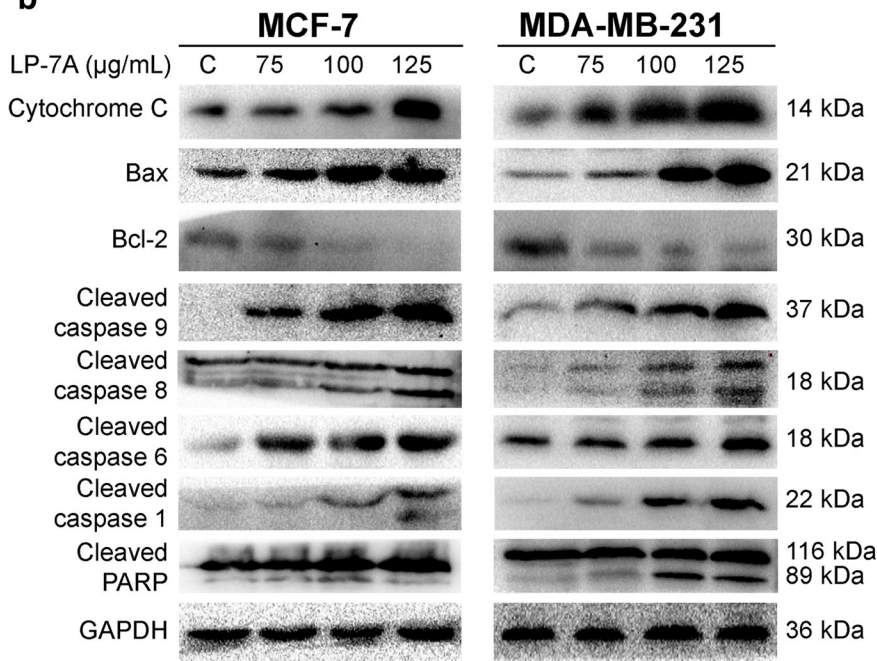
LP-7A promotes autophagy in MCF-7 and MDA-MB-231 cells

Both cell lines were treated with various concentrations (0 μg/mL, 75 μg/mL, 100 μg/mL, and 125 μg/mL) of LP-7A for 48 h, which were then analyzed for acridine orange-based autophagy assay. It is basic organic dye with the capability of penetrating through lipid bilayer membranes and emits light waves that fall into green color wavelength in a neutral environment. But in case of autophagy vacuolization, the color is turned into even lighter wavelength observed as orange or greenish orange color. We observed that the orange color is increased gradually in LP-7A-treated breast cancer cell lines across the increasing concentration (Fig. 6A and B). Furthermore, the confirmation of autophagy was evaluated by performing Western blot and analyzing the expression of the autophagy-associated proteins, i.e., Beclin-I, Atg7, Atg12, Atg5, LC3, and p62. Beclin-I is a tumor suppressor protein that regulates autophagy, LC3, and Atg's are involved in the development of autophagosomes, p62, which binds to autophagosomal units having LC3/Atg and is degraded during the autophagic process, thus making them potential markers for autophagy. The expression of autophagy-associated proteins was found higher during Western blot in LP-7A-treated breast cancer cells except for p62, which was decreased due to
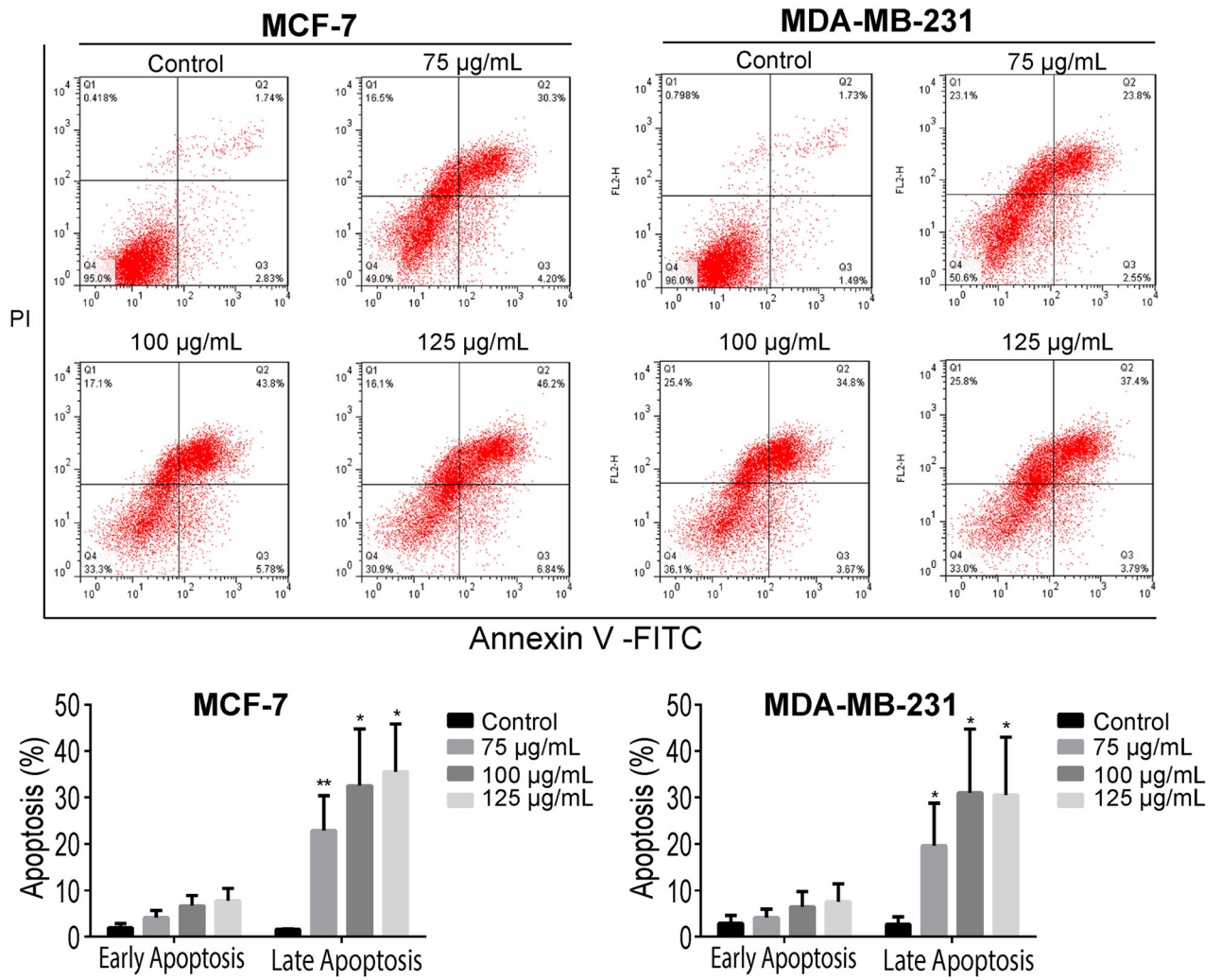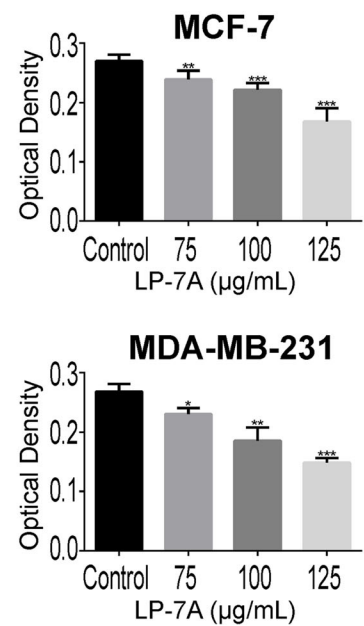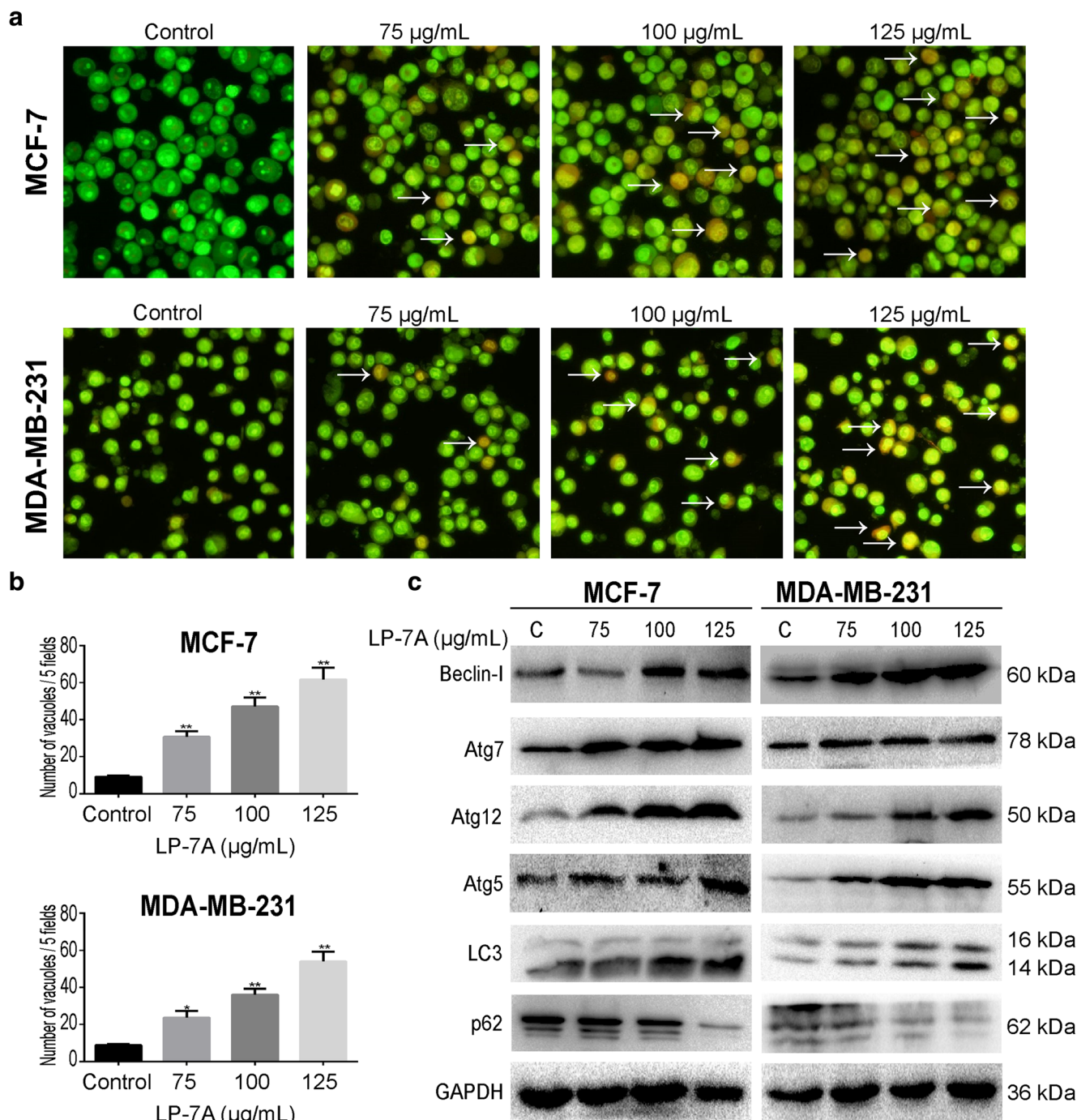
Fig. 6 LP-7A induces autophagy in breast cancer cell lines. **A and B** The role of LP-7A in the induction of autophagy is analyzed by performing acridine orange staining of MCF-7 and MDA-MB-231 cells under various indicated concentrations of LP-7A. **C** Analysis of expression of autophagy-related markers such as Beclin-I, Atg 7, Atg 12, Atg 5, LC3 I/II, and p62 was evaluated via Western blot by treating breast cancer cells with different doses (control (0 μg/mL) indicated as C, 75 μg/mL, 100 μg/mL, 125 μg/mL) of LP-7A for 48 h. Statistical analysis was performed using multiple t test via GraphPad Prism 6.0 (* $p < 0.05$, ** $p < 0.01$)

its degradation (Fig. 6C). The expression of these autophagosome membrane-associated proteins, together with acridine orange staining, gave us significant evidence that the treatment of LP-7A induces autophagy in these breast cancer cells.

Discussion

Breast cancer is linked with many deaths across the globe; therefore, it is needed to develop effective and novel therapeutic agents that can help in the control and treatment of highly

progressive tumors with minimal side effects (Ballazhi et al. 2017; Porter 2008). Latcripin-1(LP-1) from *Lentinula edodes*, are effective and efficient in terms of arresting cancer cell growth (Batool et al. 2018). However, the effect of LP-7A is not evaluated in any cancer type so far. Hence, it was our keen interest to study its effectiveness in cancer. Since the work on latcripins (LPs), other than LP-7A, as an anti-cancer agent has already been performed on other cancer types, we have selected breast cancer cells as it has not been evaluated and requires our attention due to its high incidence worldwide. We have found that LP-7A is a much efficient candidate to be useful for addressing the proliferation of aggressive cancer cells without affecting normal cells with IC_{50} around 91 μg/mL for MCF-7 and 122 μg/mL in MDA-MB-231 cells. The IC_{50} for MCF-10A, i.e., 1.8 mg/mL, represents less toxicity to normal breast cells. It has been found that the normal cell lines were less sensitive in comparison with the cancer cell lines in response to lower doses of LP-7A. However, at higher doses, the LP-7A can affect the proliferation of MCF-10A. Due to the lack of tumorigenic properties, these cells exhibit stable and non-aggressive growth patterns. The reason for this selective targeting of LP-7A may be in relation to the high proliferative properties of cancer cells. The higher sensitivity of cancer cells (MCF-7 and MDA-MB-231) towards LP-7A might be associated with their aggressive growth, as compared with MCF-10A, as well as more frequent uptake of LP-7A (Fig. 1A). Such high sensitivity of breast cancer cells towards LP-7A not only affected proliferation but also its metastatic capability. We also reported changes in morphology in breast cancer cells while such changes were not prominently seen in the MCF-10A cell line (Fig. 1B).

Furthermore, colony assay has shown a significant reduction in the formation of colonies with higher doses of LP-7A (Fig. 1C). Previous reports on the anti-cancer activity of peptides extracted from *Lentinula edodes* have also shown considerable less toxicity on normal cells (Ann et al. 2014; Batool et al. 2018; Liu et al. 2012). However, we suggest that comprehensive comparative investigations on the cytotoxicity of LP-7A and current anti-cancer drugs in high proliferative normal cells, such as dermal papillae cells and keratinocytes, are still required for further evaluation of the specificity of LP-7A.

Reports and studies have suggested that the upregulation of NF-κB serves as a proliferating agent in cancer cells (Hernandez et al. 2020; Ramamoorthy et al. 2020; Teixeira et al. 2020) and is reported to be involved in multiple roles, which include angiogenesis and metastasis as in migration and invasion (Altomare and Testa 2005; Mook et al. 2004). It has been reported that usually IKB and NF-κB form a complex and stays in an inactive state, but with the phosphorylation of IKB, NF-κB is free and can act as a transcription factor for the transcription of a variety of genes (Lin et al. 2007; Samuels et al. 2004). Such signaling makes the cancer cell express more MMPs into the matrix resulting in the transformation

of a tumor into aggressive metastatic nature (Kim et al. 2012; Luo et al. 2005). In this report, we have found that inhibition of matrix dissolving protein (MMP-2 and MMP-9) expression is down-regulated via NF-κB by LP-7A, resulting in significantly lower migration and invasion (Fig. 2B and C) and lower filling rate of scratched space during wound healing (Fig. 2A). The breast cancer cells (MCF-7 and MDA-MB-231) have shown a significant decrease in migration and invasion when treated with LP-7A. Addressing the metastasis in cancer is one of the critical factors in cancer treatment, which can result in rapid recovery (Han et al. 2004; Han et al. 2005). Such morphological changes, inhibition of growth, and a higher level of cleaved PARP (Fig. 5B) were further evaluated by the chromatin cleavage (Fig. 3A) and agarose DNA analysis (Fig. 3B), suggesting the possible nuclear chromatin and genome disability.

The activation of NF-κB also involves in the regulation of anti-apoptotic proteins such as cyclin-D1, Bcl-2, and angiogenic genes such as vascular endothelial growth factors (VEGF) (Garcia-Rostan et al. 2005; Li et al. 2005). In other cancer types such as lung cancer, the inhibition as well as nuclear translocation of NF-κB also facilitated apoptosis (Chen et al. 2011). Therefore, anti-cancer drugs which inhibit the activation of NF-κB are proved to be effective anti-cancer therapeutic agents (Li et al. 2005). Herein, our study on LP-7A-treated breast cancer cells have shown a significant increase in p21 that acts as an inhibitor for cyclin-Cdk complex and provided a substantial reduction in cyclin D1, cdk6, and cyclin E1, causing cell cycle arrest at G1 phase (Fig. 4). Additionally, for the transition of G1 phase into S phase, cyclin-Cdk plays a significant role (Chambard et al. 2007).

Furthermore, the cell inhibitory effect might also stimulate mitochondrial-mediated apoptosis, as mentioned above, the role of NF-κB in the expression of Bcl-2. Therefore, we further evaluated the influence of LP-7A to analyze the apoptosis of breast cancer cells via flow cytometry. It was of no surprise to observe the accumulation of a significantly higher percentage of apoptotic cells in the upper right (annexin V+/PI+), showing an increase in late apoptosis. Moreover, a higher number of necrotic cells in the treated groups of MCF-7 and MDA-MB-231 may suggest the efficacy of LP-7A, which destabilized these cancer cells enough to be damaged by external stresses during flow cytometry experiments (Fig. 5A). The significant expressions of caspases mediated via Bax/Bcl-2 ratio during mitochondrial stress are evident by the level of cytochrome c in breast cancer cells (Fig. 5B).

Dysregulation in cell cycle phases has been presented to be one of the main reasons to initiate apoptosis (Li and Brooks 1999). However, due to positive acridine orange stain in LP-7A-treated breast cancer cells (Fig. 6A) and increase in Beclin-1, Atg's, LC3 I/II, along with lower p62 expression (Fig. 6C) indicated autophagy in a significant number that cannot be ignored. Studies have found that autophagy may

contribute to the cell cycle arrest or vice versa (Chen et al. 2013; She et al. 2017; Tasdemir et al. 2007). Therefore, due to the novelty of LP-7A, at this moment, it is unclear that the dysregulation of the cell cycle, in LP-7A-treated cells, triggered autophagy, apoptosis, or simultaneously both or may exist a separate underlying mechanism to initiate autophagy and apoptosis. The complete mode of action of LP-7A in terms of breast cancer cell apoptosis and autophagy is yet to be evaluated. But with our current data, we conclude that it acts as a promising anti-cancer agent that can initiate intrinsic apoptosis and autophagy in breast cancer cells (MCF-7 and MDA-MB-231) mediated via mitochondrial stress. It is essential to consider that despite the difference in estrogen receptor (ER) expression in MCF-7 (ER$^+$) and MDA-MB-231 (ER$^-$), both breast cancer cell lines share the similarity, in terms of cytotoxicity of LP-7A, through NF-κB. Previous studies showed that malignancies like melanoma, leukemia, pancreatic cancer, colon cancer, and breast cancer have abnormally higher NF-κB expression (Karin 2006). The presented study on LP-7A also showed significant control over the upregulation of NF-κB. It can further be evaluated alongside with already known antitumor agents, and elaborative therapeutic implications can also be explored after tangible animal and preclinical trials.

Authors' contribution Conceptualization: S.R.U.D. and M.Z. Formal analysis: M.A.N. and M.Z.S. Investigation: S.R.U.D. Writing the first draft: M.A.N. and M.Z.S. Technical assistance: A.H., K.H.K., S.K., G.A., X.L., W.Z., X.W., A.N., and G.C. Review and editing: M.A.N and M.Z.S. Resources and supervision: M.H.

Compliance with ethical standards

Conflict of interest The authors declare that they have no conflict of interests.

Ethical approval This article does not contain any studies with animals performed by any of the authors.

References

Altomare DA, Testa JR (2005) Perturbations of the AKT signaling pathway in human cancer. Oncogene 24(50):7455–7464. https://doi.org/10.1038/sj.onc.1209085

Anderson BO, Yip CH, Smith RA, Shyyan R, Sener SF, Eniu A, Carlson RW, Azavedo E, Harford J (2008) Guideline implementation for breast healthcare in low-income and middle-income countries: overview of the breast health global initiative global summit 2007. Cancer 113(8 Suppl):2221–2243. https://doi.org/10.1002/cncr.23844

Ann XH, Lun YZ, Zhang W, Liu B, Li XY, Zhong MT, Wang XL, Cao J, Ning AH, Huang M (2014) Expression and characterization of protein latcripin-3, an antioxidant and antitumor molecule from *Lentinula edodes* C91-3. Asian Pac J Cancer Prev 15(12):5055–5061. https://doi.org/10.7314/apjcp.2014.15.12.5055

Balasubramanian K, Mirnikjoo B, Schroit AJ (2007) Regulated externalization of phosphatidylserine at the cell surface: implications for apoptosis. J Biol Chem 282(25):18357–18364. https://doi.org/10.1074/jbc.M700202200

Ballazhi L, Imeri F, Jashari A, Popovski E, Stojkovic G, Dimovski AJ, Mikhova B, Mladenovska K (2017) Original research paper. Hydrazinyldiene-chroman-2,4-diones in inducing growth arrest and apoptosis in breast cancer cells: synergism with doxorubicin and correlation with physicochemical properties. Acta Pharma 67(1):35–52. https://doi.org/10.1515/acph-2017-0006

Batool S, Joseph TP, Hussain M, Vuai MS, Khinsar KH, Din SRU, Padhiar AA, Zhong M, Ning A, Zhang W, Cao J, Huang M (2018) LP1 from *Lentinula edodes* C91-3 induces autophagy, apoptosis and reduces metastasis in human gastric cancer cell line SGC-7901. Int J Mol Sci 19(10):2986. https://doi.org/10.3390/ijms19102986

Bisen PS, Baghel RK, Sanodiya BS, Thakur GS, Prasad GB (2010) *Lentinus edodes*: a macrofungus with pharmacological activities. Curr Med Chem 17(22):2419–2430. https://doi.org/10.2174/092986710791698495

Chambard JC, Lefloch R, Pouyssegur J, Lenormand P (2007) ERK implication in cell cycle regulation. Biochim Biophys Acta 1773(8):1299–1310. https://doi.org/10.1016/j.bbamcr.2006.11.010

Chen W, Li Z, Bai L, Lin Y (2011) NF-kappaB in lung cancer, a carcinogenesis mediator and a prevention and therapy target. Front Biosci (Landmark Ed) 16:1172–1185. https://doi.org/10.2741/3782

Chen T, Hao J, He J, Zhang J, Li Y, Liu R, Li L (2013) Cannabisin b induces autophagic cell death by inhibiting the AKT/mTOR pathway and S phase cell cycle arrest in HepG2 cells. Food Chem 138(2–3):1034–1041. https://doi.org/10.1016/j.foodchem.2012.11.102

Ferlay J, Shin HR, Bray F, Forman D, Mathers C, Parkin DM (2010) Estimates of worldwide burden of cancer in 2008: GLOBOCAN 2008. Int J Cancer 127(12):2893–2917. https://doi.org/10.1002/ijc.25516

Garcia-Rostan G, Costa AM, Pereira-Castro I, Salvatore G, Hernandez R, Hermsem MJ, Herrero A, Fusco A, Cameselle-Teijeiro J, Santoro M (2005) Mutation of the PIK3CA gene in anaplastic thyroid cancer. Cancer Res 65(22):10199–10207. https://doi.org/10.1158/0008-5472.CAN-04-4259

Han SS, Kim K, Hahm ER, Lee SJ, Surh YJ, Park HK, Kim WS, Jung CW, Lee MH, Park K, Yang JH, Yoon SS, Riordan NH, Riordan HD, Kimler BF, Park CH, Lee JH, Park S (2004) L-ascorbic acid represses constitutive activation of NF-kappaB and COX-2 expression in human acute myeloid leukemia, HL-60. J Cell Biochem 93(2):257–270. https://doi.org/10.1002/jcb.20116

Han SS, Kim K, Hahm ER, Park CH, Kimler BF, Lee SJ, Lee SH, Kim WS, Jung CW, Park K, Kim J, Yoon SS, Lee JH, Park S (2005) Arsenic trioxide represses constitutive activation of NF-kappaB and COX-2 expression in human acute myeloid leukemia, HL-60. J Cell Biochem 94(4):695–707. https://doi.org/10.1002/jcb.20337

Hernandez H, Roberts AL, McDowell CM (2020) Nuclear factor-kappa beta signaling is required for transforming growth factor beta-2 induced ocular hypertension. Exp Eye Res 191:107920. https://doi.org/10.1016/j.exer.2020.107920

Jong SC, Birmingham JM (1993) Medicinal and therapeutic value of the shiitake mushroom. Adv Appl Microbiol 39:153–184. https://doi.org/10.1016/s0065-2164(08)70595-1

Joseph TP, Chanda W, Padhiar AA, Batool S, LiQun S, Zhong M, Huang M (2018) A preclinical evaluation of the antitumor activities of edible and medicinal mushrooms: a molecular insight. Integr

Cancer Ther 17(2):200–209. https://doi.org/10.1177/1534473417736861

Karin M (2006) Nuclear factor-kappaB in cancer development and progression. Nature 441(7092):431–436. https://doi.org/10.1038/nature04870

Kim YN, Koo KH, Sung JY, Yun UJ, Kim H (2012) Anoikis resistance: an essential prerequisite for tumor metastasis. Int J Cell Biol 2012: 306879–306811. https://doi.org/10.1155/2012/306879

Li JM, Brooks G (1999) Cell cycle regulatory molecules (cyclins, cyclin-dependent kinases and cyclin-dependent kinase inhibitors) and the cardiovascular system; potential targets for therapy? Eur Heart J 20(6):406–420. https://doi.org/10.1053/euhj.1998.1308

Li VS, Wong CW, Chan TL, Chan AS, Zhao W, Chu KM, So S, Chen X, Yuen ST, Leung SY (2005) Mutations of PIK3CA in gastric adenocarcinoma. BMC Cancer 5:29. https://doi.org/10.1186/1471-2407-5-29

Li T, Mello-Thoms C, Brennan PC (2016) Descriptive epidemiology of breast cancer in China: incidence, mortality, survival and prevalence. Breast Cancer Res Treat 159(3):395–406. https://doi.org/10.1007/s10549-016-3947-0

Lin HL, Yang MH, Wu CW, Chen PM, Yang YP, Chu YR, Kao CL, Ku HH, Lo JF, Liou JP, Chi CW, Chiou SH (2007) 2-Methoxyestradiol attenuates phosphatidylinositol 3-kinase/Akt pathway-mediated metastasis of gastric cancer. Int J Cancer 121(11):2547–2555. https://doi.org/10.1002/ijc.22963

Liu B, Zhong M, Lun Y, Wang X, Sun W, Li X, Ning A, Cao J, Zhang W, Liu L, Huang M (2012) A novel apoptosis correlated molecule: expression and characterization of protein Latcripin-1 from Lentinula edodes C(91-3). Int J Mol Sci 13(5):6246–6265. https://doi.org/10.3390/ijms13056246

Luo JL, Kamata H, Karin M (2005) IKK/NF-kappaB signaling: balancing life and death–a new approach to cancer therapy. J Clin Invest 115(10):2625–2632. https://doi.org/10.1172/JCI26322

Mook OR, Frederiks WM, Van Noorden CJ (2004) The role of gelatinases in colorectal cancer progression and metastasis. Biochim Biophys Acta 1705(2):69–89. https://doi.org/10.1016/j.bbcan.2004.09.006

Padhiar AA, Chanda W, Joseph TP, Guo X, Liu M, Sha L, Batool S, Gao Y, Zhang W, Huang M, Zhong M (2018) Comparative study to develop a single method for retrieving wide class of recombinant proteins from classical inclusion bodies. Appl Microbiol Biotechnol 102(5):2363–2377. https://doi.org/10.1007/s00253-018-8754-6

Porter P (2008) "Westernizing" women's risks? Breast cancer in lower-income countries. N Engl J Med 358(3):213–216. https://doi.org/10.1056/NEJMp0708307

Ramamoorthy A, Mahendra J, Mahendra L, Govindaraj J, Samu S (2020) Effect of sudharshan kriya pranayama on salivary expression of human beta defensin-2, peroxisome proliferator-activated receptor gamma, and nuclear factor-kappa b in chronic periodontitis. Cureus 12(2):e6905. https://doi.org/10.7759/cureus.6905

Rincao VP, Yamamoto KA, Ricardo NM, Soares SA, Meirelles LD, Nozawa C, Linhares RE (2012) Polysaccharide and extracts from Lentinula edodes: structural features and antiviral activity. Virol J 9: 37. https://doi.org/10.1186/1743-422X-9-37

Samuels Y, Wang Z, Bardelli A, Silliman N, Ptak J, Szabo S, Yan H, Gazdar A, Powell SM, Riggins GJ, Willson JK, Markowitz S, Kinzler KW, Vogelstein B, Velculescu VE (2004) High frequency of mutations of the PIK3CA gene in human cancers. Science 304(5670):554. https://doi.org/10.1126/science.1096502

She T, Feng J, Lian S, Li R, Zhao C, Song G, Luo J, Dawuti R, Cai S, Qu L, Shou C (2017) Sarsaparilla (Smilax Glabra rhizome) extract activates redox-dependent ATM/ATR pathway to inhibit cancer cell growth by S phase arrest, apoptosis, and autophagy. Nutr Cancer 69(8):1281–1289. https://doi.org/10.1080/01635581.2017.1362447

Tasdemir E, Maiuri MC, Tajeddine N, Vitale I, Criollo A, Vicencio JM, Hickman JA, Geneste O, Kroemer G (2007) Cell cycle-dependent induction of autophagy, mitophagy and reticulophagy. Cell Cycle 6(18):2263–2267. https://doi.org/10.4161/cc.6.18.4681

Teixeira LFS, Peron JPS, Bellini MH (2020) Silencing of nuclear factor kappa b 1 gene expression inhibits colony formation, cell migration and invasion via the downregulation of interleukin 1 beta and matrix metallopeptidase 9 in renal cell carcinoma. Mol Biol Rep 47(2): 1143–1151. https://doi.org/10.1007/s11033-019-05212-9

Wyllie AH (1980) Glucocorticoid-induced thymocyte apoptosis is associated with endogenous endonuclease activation. Nature 284(5756): 555–556. https://doi.org/10.1038/284555a0

Wyllie AH, Kerr JF, Currie AR (1980) Cell death: the significance of apoptosis. Int Rev Cytol 68:251–306. https://doi.org/10.1016/s0074-7696(08)62312-8